Correlation function and susceptibility of site- and bond-diluted Heisenberg paramagnets

Kazuko Kawasaki*
Department of Physics, Nara Women's University, Nara, 630 Japan

Raza A. Tahir-Kheli*
Department of Physics, Temple University, Philadelphia, Pennsylvania 19122
and J. Stefan Institute, University of Ljubljana, Jamova 39, 61001 Ljubljana, Yugoslavia †

(Received 23 July 1976)

Generalizing the recent work of Collins, the wave-vector-dependent susceptibility and the static correlation function for a randomly diluted Heisenberg paramagnet on a Bravais lattice with quenched-site, or nearest-neighbor exchange-bond, dilution is studied by high-temperature series-expansion techniques. The first five coefficients for the spin correlation function $S(\vec{k})$ and susceptibility $\chi(\vec{k})$ are calculated for arbitrary $\vec{k}$, the sign of the exchange and the spin magnitude and the magnetic site c and bond p concentrations. Numerical results for these functions are presented for various spins and for $\vec{k}$ along the symmetry directions (1,1,1) and (1,0,0). Because of the generality of the present series, their length is rather limited, and as such they are not suitable for a careful analysis of the critical region. Nonetheless, to get a qualitative feel for the accuracy of the present results near the transition region, we have used Padé approximants for determining the correlation length $\xi(T)$ as a function of the reduced temperature $\epsilon = [T - T_{C(N)}(\text{random})]/T_{C(N)}(\text{random})$. In this manner, we estimate that the numerical accuracy of our results should be reasonable as long as the system is moderately above the transition temperature, e.g., $\epsilon \gtrsim 0.5$.

I. INTRODUCTION

The dynamics of randomly diluted Heisenberg ferro- and antiferromagnets with quenched in site and bond dilution has been analyzed at low temperatures in the coherent-potential approximation by several authors.[1-3] In the opposite limit of high temperatures, we have recently given an approximate description of the same by a phenomenological procedure which makes use of the first four frequency moments of the correlation function, which are determined in the limit of infinite temperature where magnetic short-range order is vanishing.[4]

For finite temperatures, however, the paramagnetic short-range order is of central importance. Here, only the statics of the random system has been studied. The procedure consists in analyzing the high-temperature series expansion for the $\vec{k}=\vec{Q}$ susceptibility.[5,6] Corresponding work for arbitrary wave vectors is available only for the nonrandom, undiluted ("pure") system.[7]

In the present paper we generalize Collins's[7] study of the wave-vector-dependent properties of the pure Heisenberg paramagnet to arbitrary bond or site dilution. In other words, we work either with a system where the concentration of sites occupied by magnetic atoms is c $(0<c\leq 1)$ or where the concentration of connected nearest-neighbor bonds is p $(0<p\leq 1)$. The relevant, configuration-dependent Hamiltonian is written

$$\mathcal{H}_{\text{config}} = -\sum_{ij} p_{ij} J(ij) c_i c_j \vec{S}_i \cdot \vec{S}_j . \tag{1.1}$$

The given distribution of the magnetic sites (or the connected bonds) is specified by the random variables c_i (or p_{ij}), which are the usual site (or bond) occupation operators such that c_i is unity if site i is occupied by a magnetic atom (or, $p_{ij}=1$ if the exchange bond ij is connected); otherwise, they are zero. Also $J(ij)=\pm J$ only if i and j are neighboring sites and the upper and lower signs imply ferro- and antiferromagnetic coupling, respectively. The magnitude of the spin $S(\hbar=1)$ is arbitrary as are the site (or bond) concentrations c (or p).

The wavelength-dependent susceptibility $\chi(\vec{k})$, and correlation function $S(\vec{k})$ are defined as

$$\chi^{\alpha\alpha}(\vec{k}) = g^2\mu^2\beta \sum_{\{c,p\}} \sum_f e^{-i\vec{k}\cdot\vec{f}} \int_0^1 d\lambda \, \langle c_0 S_0^\alpha c_f S_f^\alpha (i\beta\lambda)\rangle_{\text{config}} \tag{1.2}$$

and

$$S^{\alpha\alpha}(\vec{k}) = \sum_{\{c,p\}} \sum_f e^{-i\vec{k}\cdot\vec{f}} \langle c_0 S_0^\alpha c_f S_f^\alpha \rangle_{\text{config}} , \tag{1.3}$$

where $\beta=(k_BT)^{-1}$, μ is the Bohr magneton, and g the gyromagnetic ratio. The superscript α denotes x, y, or z, component of the spin. [Because of spatial isotropy of the Hamiltonian (1.1) in the paramagnetic region, both the susceptibility and the correlation function are independent of the superscript α. As such, for convenience, this superscript can, without any ambiguity, be dropped.] Both the complex time dependence of the spin operators in Eq. (1.2) (specified in the Heisenberg representation) and the canonical averages, de-

noted by pointed brackets with subscript "config," are with respect to the configuration-dependent Hamiltonian given in Eq. (1.1). Finally, we note here that because we are dealing with quenched spatial disorder, it is essential that in order to achieve appropriate thermodynamic averaging, the weighted summation over all the possible configurations, consistent with given concentration c (or p) of magnetic sites (or bonds, as the case may be) denoted by

$$\sum_{\{c,p\}}',$$

be carried out last.

In order to get a qualitative measure of the magnetic short-range order, we expand the correlation function $S(\vec{k})$ in a Taylor expansion about the magnetic reciprocal-lattice vector $\vec{Q}$ of the given system, i.e., $\vec{Q}=(q,q,q)$, where for a ferromagnet $q=0$; $q=\pi$ for an antiferromagnet of sc lattice structure and 2π for that of bcc or fcc structure (we choose our units such that the primitive cube edge a, is of unit length):

$$S(\vec{k})=S(\vec{Q})[1\mp\xi^2(T)|\vec{k}-\vec{Q}|^2+O(|\vec{k}-\vec{Q}|^4)]. \quad (1.4)$$

Recasting this in the Ornstein-Zernike form, the following asymptotic form is obtained:

$$S(\vec{k})\simeq S(\vec{Q})K^2(T)/[K^2(T)\pm|\vec{k}-\vec{Q}|^2], \quad (1.5)$$

where the upper and the lower signs correspond, respectively, to the cases of ferro- and antiferromagnetic exchange coupling and where $K(T)=1/\xi(T)$. By Fourier inversion, this gives the expression

$$S(\vec{r})\simeq(e^{-Kr}/r)e^{-i\vec{Q}\cdot\vec{r}}. \quad (1.6)$$

In this fashion the quantity $\xi(T)$ emerges as a natural measure of the effective correlation length. As is well known, the correlation length diverges as the critical temperature is approached. Away from the critical region, the correlation length is finite, approaching zero at $T=\infty$. Thus, it also provides a convenient measure of the short-range order effects in the paramagnetic phase.

II. SERIES EXPANSION

When the wavelength-dependent susceptibility $\chi(\vec{k})$ and the correlation function $S(\vec{k})$ are studied by the high-temperature series-expansion technique,[7] they are written

$$\chi(\vec{k})=Ng^2\mu^2\beta\sum_{n=0}^{\infty}X_n\Theta^{-n} \quad (2.1)$$

and

$$S(\vec{k})=\sum_{n=0}^{\infty}S_n\Theta^{-n}, \quad (2.2)$$

where Θ is a dimensionless reduced temperature — defined as the ratio $\pm k_BT/|J|$. For the system being considered here, the standard procedure for computation of the high-temperature series expansion,[7] has to be generalized so as to deal with the additional feature of spatial randomness. For instance, the coefficient S_n in Eq. (2.2) is now given as

$$S_n=\frac{(-1)^n}{n!}\sum_{\{c,p\}}'\langle\langle c_0S_0c_fS_f\mathcal{H}^n\rangle_\infty\rangle_{\text{config}}. \quad (2.3)$$

Here the canonical expectation value, denoted as $\langle\cdots\rangle_\infty$, has to be evaluated (in the infinite-temperature limit) for the given configuration: the configuration average, over all possible such configurations, is taken next.

We have evaluated the first five coefficients in this series expansion for $\chi(\vec{k})$ and $S(\vec{k})$ for arbitrary Bravais lattice, i.e., for sc, bcc, and fcc lattices. These results have been checked by making comparisons with available results relevant to several limiting cases. We have compared our results for the site-diluted problem in the $\vec{k}=0$ limit with those given by Morgan and Rushbrooke.[5] For the pure Heisenberg system (i.e., $c=p=1$), we found our results for arbitrary $\vec{k}$ values to be identical to those of Collins[7] and finally for the bond-diluted system our results were checked against the available $S=\frac{1}{2}$, $\vec{k}=0$ results given by Brown *et al.*[6]

The final expressions for the coefficients X_n for $\chi(\vec{k})$ and S_n for $S(\vec{k})$ are given in the following:

(a) First, we present the results for the site-diluted system:

$$\begin{aligned}
&X_0=cx,\quad X_1=2c^2x^2\Sigma_1,\quad X_2=-\tfrac{2}{3}zc^2x^2-\tfrac{1}{3}c^2x^2\Sigma_1+4c^3x^3\Sigma_2,\\
&X_3=\tfrac{1}{3}zc^2x^2-\tfrac{4}{3}zp_1c^3x^3+[\tfrac{1}{15}(-72x^2-24x+3)c^2x^2-\tfrac{8}{3}(z-1)c^3x^3]\Sigma_1-\tfrac{4}{3}c^3x^3\Sigma_2+8c^4x^4\Sigma_3,\\
&X_4=z\{\tfrac{1}{5}(8x^2+4x-1)+\tfrac{1}{5}[6(z-1)+4p_1]cx-\tfrac{8}{3}p_2c^2x^2\}c^2x^2\\
&\quad+\{\tfrac{1}{5}(12x^2+6x-\tfrac{2}{3})+[-\tfrac{144}{5}x^2p_1-\tfrac{48}{5}xp_1+2(z-1)+\tfrac{2}{5}p_1]cx+16(1-\tfrac{1}{3}z)p_1c^2x^2\}c^2x^2\Sigma_1\\
&\quad+[\tfrac{1}{5}(-96x^2-32x+\tfrac{14}{3})-\tfrac{8}{3}(3z-4)cx]c^3x^3\Sigma_2-4c^4x^4\Sigma_3+16c^5x^5\Sigma_4;
\end{aligned} \quad (2.4a)$$

$$S_0 = cx\,,\quad S_1 = 2c^2x^2\Sigma_1\,,\quad S_2 = -c^2x^2\Sigma_1 + 4c^3x^3\Sigma_2\,,$$
$$S_3 = [\tfrac{8}{15}(-9x^2-3x+1) + \tfrac{4}{3}(2-2z-p_1)cx]c^2x^2\Sigma_1 - \tfrac{4}{3}c^3x^3\Sigma_2 + 8c^4x^4\Sigma_3\,,$$
$$S_4 = \{-\tfrac{1}{3}(-12x^2-6x+1) + [-\tfrac{144}{5}p_1x^2 - \tfrac{48}{5}p_1x + \tfrac{10}{3}(z-1) + \tfrac{6}{5}p_1]cx - \tfrac{8}{3}[2(z-3)p_1 + p_2]c^2x^2\}c^2x^2\Sigma_1 \qquad (2.4b)$$
$$+ [-\tfrac{4}{5}(24x^2+8x-1) - \tfrac{8}{3}(3z-4)cx]c^3x^3\Sigma_2 - 4c^4x^4\Sigma_3 + 16c^5x^5\Sigma_4\,.$$

(b) The corresponding results for the bond diluted case are

$$X_0 = x\,,\quad X_1 = 2px^2\Sigma_1\,,\quad X_2 = -\tfrac{2}{3}zpx^2 - \tfrac{1}{3}px^2\Sigma_1 + 4p^2x^3\Sigma_2\,,$$
$$X_3 = \tfrac{1}{3}z(1-4p_1p^2x)px^2 + \{\tfrac{1}{5}(-24x^2-8x+1) + \tfrac{4}{3}[-2(z-1)px]\}px^2\Sigma_1 - \tfrac{4}{3}p^2x^3\Sigma_2 + 8p^3x^4\Sigma_3\,,$$
$$X_4 = \tfrac{1}{5}z[(8x^2+4x-1) + 6(z-1)px + 4p_1p^2x - \tfrac{40}{3}p_2p^3x^2]px^2 \qquad (2.5a)$$
$$+ \tfrac{1}{5}\{(12x^2+6x-\tfrac{2}{3}) + 10(z-1)px + p_1p^2x[-144x^2 - \tfrac{64}{3}x + 2 - \tfrac{80}{3}(z-2)px]\}px^2\Sigma_1$$
$$+ [\tfrac{1}{5}(-96x^2-32x+\tfrac{14}{3}) - \tfrac{8}{3}(3z-4)px]p^2x^3\Sigma_2 - 4p^3x^4\Sigma_3 + 16p^4x^5\Sigma_4\,;$$
$$S_0 = x\,,\quad S_1 = 2px^2\Sigma_1\,,\quad S_2 = -px^2\Sigma_1 + 4p^2x^3\Sigma_2\,,$$
$$S_3 = \tfrac{4}{3}[\tfrac{2}{5}(-9x^2-3x+1) - 2(z-1)px - p_1p^2x]px^2\Sigma_1 - \tfrac{4}{3}p^2x^3\Sigma_2 + 8p^3x^4\Sigma_3\,,$$
$$S_4 = \tfrac{1}{3}[(12x^2+6x-1) + 10(z-1)px + \tfrac{2}{5}p_1(-216x^2-32x+9)p^2x - 8(2zp_1 - 4p_1 + p_2)p^3x^2]px^2\Sigma_1 \qquad (2.5b)$$
$$+ [\tfrac{4}{5}(-24x^2-8x+1) - \tfrac{8}{3}(3z-4)px]p^2x^3\Sigma_2 - 4p^3x^4\Sigma_3 + 16p^4x^5\Sigma_4\,.$$

We remind ourselves that here we are dealing with a system with quenched in randomness involving site or bond dilution. The lower case c and p denote the relative concentrations of the magnetic atoms and connected exchange bonds, respectively, and $x = \frac{1}{3}S(S+1)$. Other notation is the same as that used by Collins,[7] with z being the coordination number of the magnetic lattice and p_n the number of closed nonintersecting circuits of $(n+2)$ neighboring atoms involving both a given atom and a particular one of its nearest neighbors. Relevant to the lattices considered here, i.e., sc, bcc, and fcc, these quantities are listed in Table I. Finally, here Σ_n denotes the sums of cosines of the scalar product of $\vec{k}$ and, starting from the origin, the end points of all the nonintersecting walks of n steps leading to neighboring atoms. These sums are rather tedious and for convenience they are enumerated for lattices of cubic symmetry, in the Appendix.

Correlation length. Collins[7] has given high-temperature series expansion for the spin-correlation length defined in our Eqs. (1.4)–(1.6). It is interesting to examine how the series expression for the spin-correlation length $\xi(T)$ varies with spatial randomness caused by magnetic (site and bond) dilution. To this end, in the following we generate the appropriate series expansion for $\xi(T)$.

As is evident from the structure of the series expansion for the correlation function given above, the wave-vector dependence of $S(\vec{k})$ enters through the factors Σ_n, for which detailed expressions are recorded in the Appendix. Because we need to represent $S(\vec{k})$ in a Taylor's expansion around the magnetic inverse lattice wave vectors $\vec{Q}$, it is convenient first to write

$$\Sigma_n = \Sigma_n' - \Sigma_n''|\vec{Q}-\vec{k}|^2 + O(|\vec{Q}-\vec{k}|^4)\,. \qquad (2.6)$$

The complexity of the factors Σ_n makes the generation of this expansion rather tedious. In view of the usefulness of the coefficients Σ_n' and Σ_n'' we have listed them in Table II.

Inserting the expression (2.6) into Eqs. (2.4b) and (2.5b) and combining them with Eqs. (1.4) and (2.2) we can write

$$\xi^2(T) = \sum_{n=1}\frac{\rho_n}{\Theta^n}\,, \qquad (2.7)$$

where Θ is as defined earlier following Eq. (2.2) and where

TABLE I. Parameters z, p_1, and p_2 for cubic lattices.

	sc	bcc	fcc
z	6	8	12
p_1	0	0	4
p_2	4	12	22

TABLE II. Parameters Σ_n' and Σ_n'' for cubic lattices.

	Σ_1'	Σ_2'	Σ_3'	Σ_4'	Σ_1''	Σ_2''	Σ_3''	Σ_4''
sc	±6	30	±150	726	±1	12	±97	672
bcc	±8	56	±392	2648	±1	16	±177	1696
fcc	12	132	1404	14700	1	24	409	6012

$\rho_n = W_n$ for $J>0$, $\rho_n = W'_n$ for $J<0$.

We have listed these coefficients for lattices of cubic structure and for $S=\frac{1}{2}$ and $\frac{3}{2}$ in Table III. Note that for convenience the listed numbers have not been rounded off and moreover only five-figure numerical accuracy has been maintained.

From these tables it is evident that because the leading term in the series for $\xi^2(T)$ is proportional to the concentration (of magnetic spins or of magnetic bonds, as the case may be) and moreover is of the order Θ^{-1}, therefore the spin-correlation length approaches zero as the inverse of the system temperature and/or the magnetic concentration is reduced toward zero. Indeed, on physical grounds we know that if the magnetic concentration fell below the percolation concentration (for the given lattice), the macroscopic connectivity of the magnetic lattice would break down and as such the spin correlation length would reduce to zero. This critical feature, however, cannot be expected to be evident from the simple series expansion given here. Rather, one would need to carry out a careful Padé approximant representation of the series from which, if the series were reasonably long, such critical features may emerge. Quite obviously, the present series is too short to yield to such an analysis successfully. In our opinion, procedures for the generation of series expansions[5,6] are now sufficiently well developed to generate a series of adequate length for $\xi^2(T)$ as long as the value of the wave vector is, unlike in the present work, not kept arbitrary and the computation is focussed so that only the second moment, i.e., the terms proportional to $|\vec{k}-\vec{Q}|^2$, are computed.

III. NUMERICAL RESULTS

As stated above, our series is too short to predict with any precision the details of the various critical effects. It is, nonetheless, reasonable to inquire as to whether we can get a qualitative measure of the simplest of the critical parameters, namely the magnitude of the transition temperature and, moreover, to see how the correlation function, the susceptibility, and, if possible, the correlation length might depend upon the system randomness, the lattice connectivity, etc., in the extreme paramagnetic region where the convergence of the present series is good and also in the intermediate region to which some plausible extrapolation may be effected.

Because the available longer series[5,6] for the uniform susceptibility have been used to give reasonable estimates of the magnetic transition temperature, it is convenient to begin with the examination as to how well the corresponding estimates from our present series agree with these. In the present work we have employed the [2, 1] Padé approximant for $\chi(\vec{k}=\vec{Q})$ to compute T_C(random) from the uniform susceptibility and T_N(random) from the staggered susceptibility. In Figs. 1(a) and 1(b) we show a typical set of results.

It is clear that our estimates for the magnetic transition temperature are reasonable when impurity concentration is not too large. Indeed, looking at other lattices (not shown here) we come to the conclusion that, roughly speaking, as long as the magnetic concentration is higher than a point approximately intermediate between unity and the percolation concentration, the present estimates for transition temperatures can be assumed to be within a few percent of those one might expect to obtain from series with eight or nine terms.

It should be mentioned here that since the correlation length $\xi(T)$ is expected also to diverge at the same temperature, one might also calculate the transition temperature using the series for $\xi(T)$. Not unexpectedly, it turns out that the estimated transition temperatures from these two methods, namely the divergence of the susceptibility and the correlation length, are different. The differences between these two estimates are non-negligible for small S, though for large S the relative differences become small. (Because of the greater accuracy of the estimates provided by the susceptibility, in what follows we use these estimates unless we explicitly specify to the contrary.)

Let us examine first the generalized susceptibility. For convenience of display we normalize the susceptibility at $T\to\infty$. Figures 2(a) and 2(b) refer, respectively, to ferromagnetic coupling with site dilution and antiferromagnetic coupling with bond dilution. The wave vectors for the two plots are, respectively, along the (1, 1, 1) diagonal and the cube edge (1, 0, 0). At high temperatures the normalized susceptibility is unity for all $\vec{k}$ vectors. For finite temperatures, the susceptibility is seen to be a strong function of the wave vector, peaking at the wave vectors of the magnetic reciprocal lattice, i.e., at $\vec{k}=\vec{Q}$. Furthermore, as is well known, the susceptibility is seen to peak to higher values as temperatures are lowered toward the transition temperature. The new result of the present paper is that for given value of the ratio $T/T_{C(N)}$ the normalized susceptibility for $\vec{k}$ vectors close to $\vec{Q}$ is *higher* for the *random* system. In a sense, this result has a physical counterpart at low temperatures, where the $\vec{k}\to 0$ spin-wave stiffness is known to get softer faster than the rate of dilution as the system randomness is increased.[1,2] Because the low-temperature generalized susceptibility has an inverse relationship to the spin-wave

TABLE III. Parameters W_n and W'_n for cubic lattices, with ferro- and antiferromagnetic nearest-neighbor exchange couplings, respectively, and with site and bond randomness. Here S indicates the spin values and c and p refer to magnetic site and bond concentrations, respectively.

(a) Simple cubic–site dilution

		Ferromagnetic coupling				Antiferromagnetic coupling			
S	c	W_1	W_2	W_3	W_4	W'_1	W'_2	W'_3	W'_4
$\frac{1}{2}$	1.0	0.5000	1.2500	3.5000	4.9166	−0.500 00	1.7500	−2.5000	7.3333
	0.9	0.4499	0.9899	2.5173	2.8440	−0.4499	1.4399	−1.7073	4.4014
	0.8	0.4000	0.7600	1.7373	1.4742	−0.4000	1.1600	−1.0973	2.3849
	0.7	0.3499	0.5600	1.1366	0.6345	−0.3499	0.9099	−0.6466	1.0828
	0.6	0.3000	0.3899	0.6920	0.1755	−0.3000	0.6899	−0.3320	0.3176
	0.5	0.2500	0.2500	0.3802	−0.2864	−0.2500	0.5000	−0.1302	−0.0651
	0.4	0.1999	0.1399	0.1779	−0.8073	−0.1999	0.3399	−0.0179	−0.1960
	0.3	0.1500	0.0599	0.0621	−0.0598	−0.1500	0.2099	0.0278	−0.1827
	0.2	0.0999	0.0100	0.0093	−0.0217	−0.0999	0.1100	0.0306	−0.1090
	0.1	0.0499	−0.0100	−0.0036	0.0012	−0.0499	0.0399	0.0136	−0.0357
$\frac{3}{2}$	1.0	2.5000	36.2500	464.833	5215.416	−2.5000	38.7500	−439.833	5730.834
	0.9	2.2499	29.2499	336.270	3331.670	−2.2499	31.4999	−316.021	3699.591
	0.8	1.9999	23.0000	233.700	2005.217	−1.9999	25.0000	−217.700	2256.383
	0.7	1.7499	17.5000	154.211	1114.945	−1.7499	19.2500	−141.962	1276.564
	0.6	1.4999	12.7500	94.899	554.449	−1.4999	14.2500	−85.900	650.198
	0.5	1.2500	8.7500	52.859	231.939	−1.2500	10.0000	−46.609	281.966
	0.4	0.9999	5.5000	25.183	70.241	−0.9999	6.4999	−21.183	91.158
	0.3	0.7499	3.0000	8.965	6.807	−0.7499	3.7499	−6.715	11.698
	0.2	0.4999	1.2500	1.299	−6.283	−0.4999	1.7499	−0.300	−7.866
	0.1	0.2499	0.2499	−0.719	−2.328	−0.2499	0.4999	0.969	−4.365

(b) Simple cubic–bond dilution

S	p								
$\frac{1}{2}$	1.0	0.500 00	1.2500	3.5000	4.9166	−0.5000	1.7500	−2.5000	7.3333
	0.9	0.4499	0.9899	2.5173	2.8561	−0.4499	1.4399	−1.7073	4.3892
	0.8	0.4000	0.7600	1.7373	1.4913	−0.4000	1.1600	−1.0973	2.3678
	0.7	0.3499	0.5600	1.1366	0.6517	−0.3499	0.9099	−0.6466	1.0657
	0.6	0.3000	0.3899	0.6920	0.1899	−0.3000	0.6899	−0.3320	0.3032
	0.5	0.2500	0.2500	0.3802	−0.0182	−0.2500	0.5000	−0.1302	−0.0755
	0.4	0.1999	0.1399	0.1779	−0.0743	−0.1999	0.3399	−0.0179	−0.2024
	0.3	0.1500	0.0599	0.0621	−0.0566	−0.1500	0.2099	0.0278	−0.1858
	0.2	0.0999	0.0100	0.0093	−0.0206	−0.0999	0.1100	0.0306	−0.1101
	0.1	0.0499	−0.0100	−0.0036	0.0013	−0.0499	0.0399	0.0136	−0.0359
$\frac{3}{2}$	1.0	2.5000	36.2500	464.833	5215.416	−2.5000	38.7500	−439.833	5730.834
	0.9	2.2499	29.2499	336.270	3333.214	−2.2499	31.4999	−316.021	3698.076
	0.8	1.9999	23.0000	233.700	2007.349	−1.9999	25.0000	−217.700	2254.246
	0.7	1.7499	17.5000	154.211	1117.089	−1.7499	19.2500	−141.962	1274.420
	0.6	1.4999	12.7500	94.8999	556.249	−1.4999	14.2500	−85.900	648.398
	0.5	1.2500	8.7500	52.8593	233.242	−1.2500	10.0000	−46.609	280.663
	0.4	0.9999	5.5000	25.1832	71.041	−0.9999	6.4999	−21.183	90.358
	0.3	0.7499	3.0000	8.9656	7.201	−0.7499	3.7499	−6.715	11.304
	0.2	0.4999	1.2500	1.2999	−6.149	−0.4999	1.7499	−0.300	−7.999
	0.1	0.2499	0.2499	−0.7197	−2.309	−0.2499	0.4999	0.969	−4.383

TABLE III. *(Continued)*

(c) bcc lattice–site dilution

S	c								
$\frac{1}{2}$	1.0	0.500 0	1.7500	6.5833	15.9999	−0.5000	2.2500	−5.2500	21.6666
	0.9	0.4499	1.3950	4.7516	9.8019	−0.4499	1.8449	−3.6716	13.6611
	0.8	0.4000	1.0800	3.2946	5.5713	−0.4000	1.4800	−2.4413	8.0393
	0.7	0.3499	0.8050	2.1697	2.8485	−0.3499	1.1549	−1.5163	4.2891
	0.6	0.3000	0.5699	1.3340	1.2339	−0.3000	0.8699	−0.8540	1.9579
	0.5	0.2500	0.3750	0.7447	0.3880	−0.2500	0.6250	−0.4114	0.6536
	0.4	0.1999	0.2199	0.3593	0.0310	−0.1999	0.4199	−0.1459	0.0436
	0.3	0.1500	0.1049	0.1348	−0.0566	−0.1500	0.2549	−0.0148	−0.1443
	0.2	0.0999	0.0300	0.0286	−0.0346	−0.0999	0.1300	0.0246	−0.1226
	0.1	0.0499	−0.0050	−0.0020	−0.0256	−0.0499	0.0449	0.0153	−0.0437
$\frac{3}{2}$	1.0	2.5000	48.7500	866.916	14 128.33	−2.5000	51.2500	−833.583	15 133.33
	0.9	2.2499	39.3749	629.050	9125.14	−2.2499	41.6248	−602.051	9848.28
	0.8	1.9999	31.0000	439.033	5578.14	−1.9999	33.0000	−417.700	6077.31
	0.7	1.7499	23.6250	291.513	3174.68	−1.7499	25.3750	−275.180	3501.16
	0.6	1.4999	17.2500	181.149	1639.85	−1.4999	18.7500	−169.150	1838.35
	0.5	1.2500	11.8750	102.599	736.21	−1.2500	13.1250	−94.265	844.82
	0.4	0.9999	7.4999	50.516	263.80	−0.9999	8.5000	−45.183	314.05
	0.3	0.7499	4.1249	19.559	60.18	−0.7499	4.8749	−16.559	76.98
	0.2	0.4999	1.7500	4.383	0.400	−0.4999	2.2499	−3.050	2.06
	0.1	0.2499	0.3749	−0.355	−3.011	−0.2499	0.6249	0.688	−4.74

(d) bcc lattice–bond dilution

S	p								
$\frac{1}{2}$	1.0	0.5000	1.7500	6.5833	15.9999	−0.5000	2.2500	−5.2500	21.6666
	0.9	0.4499	1.3950	4.7516	9.8383	−0.4499	1.8449	−3.6716	13.6246
	0.8	0.4000	1.0800	3.2946	5.6225	−0.4000	1.4800	−2.4413	7.9881
	0.7	0.3499	0.8050	2.1697	2.9000	−0.3499	1.1549	−1.5163	4.2376
	0.6	0.3000	0.5699	1.3340	1.2771	−0.3000	0.8699	−0.8540	1.9148
	0.5	0.2500	0.3750	0.7447	0.4192	−0.2500	0.6250	−0.4114	0.6224
	0.4	0.1999	0.2199	0.3593	0.0502	−0.1999	0.4199	−0.1459	0.0244
	0.3	0.1500	0.1049	0.1348	−0.0472	−0.1500	0.2549	−0.0148	−0.1537
	0.2	0.0999	0.0300	0.0286	−0.0314	−0.0999	0.1300	0.0246	−0.1258
	0.1	0.0499	−0.0050	−0.0020	−0.0021	−0.0499	0.0449	0.0153	−0.0442
$\frac{3}{2}$	1.0	2.5000	48.7500	866.916	14 128.33	−2.5000	51.2500	−833.583	15 133.33
	0.9	2.2499	39.3749	629.050	9129.70	−2.2499	41.6248	−602.051	9843.73
	0.8	1.9999	31.0000	439.033	5584.54	−1.9999	33.0000	−417.700	6070.91
	0.7	1.7499	23.6250	291.513	3181.11	−1.7499	25.3750	−275.180	3494.73
	0.6	1.4999	17.2500	181.149	1645.25	−1.4999	18.7500	−169.150	1832.95
	0.5	1.2500	11.8750	102.599	740.11	−1.2500	13.1250	−94.265	840.92
	0.4	0.9999	7.4999	50.516	266.20	−0.9999	8.5000	−45.183	311.65
	0.3	0.7499	4.1249	19.559	61.37	−0.7499	4.8749	−16.559	75.80
	0.2	0.4999	1.7500	4.383	0.800	−0.4999	2.2499	−3.050	1.66
	0.1	0.2499	0.3749	−0.355	−2.955	−0.2499	0.6249	0.688	−4.80

TABLE III. *(Continued)*

(e) fcc lattice-site dilution
Ferromagnetic coupling

S	c	W_1	W_2	W_3	W_4
$\frac{1}{2}$	1.0	0.5000	2.7500	15.4166	68.9167
	0.9	0.4499	2.2050	11.1371	43.6133
	0.8	0.4000	1.7200	7.7319	25.9574
	0.7	0.3499	1.2949	5.1015	14.2405
	0.6	0.3000	0.9299	3.1460	6.9688
	0.5	0.2500	0.6250	1.7656	2.8619
	0.4	0.1999	0.3799	0.8606	0.8544
	0.3	0.1500	0.1949	0.3313	0.0947
	0.2	0.0999	0.0700	0.0779	−0.0545
	0.1	0.0499	0.0049	0.0007	−0.0164
$\frac{3}{2}$	1.0	2.5000	73.7500	2037.754	52417.86
	0.9	2.2499	59.6248	1481.238	34064.17
	0.8	1.9999	47.0000	1036.366	20996.83
	0.7	1.7499	35.8750	690.658	12091.39
	0.6	1.4999	26.2500	431.649	6358.09
	0.5	1.2500	18.1250	246.869	2940.77
	0.4	0.9999	11.5000	123.850	1117.14
	0.3	0.7499	6.3749	50.121	298.82
	0.2	0.4999	2.7500	13.216	31.31
	0.1	0.2499	0.6250	0.665	−6.03

(f) fcc-bond dilution
Antiferromagnetic coupling

S	p	W_1	W_2	W_3	W_4
$\frac{1}{2}$	1.0	0.5000	2.7500	15.4166	68.9167
	0.9	0.4499	2.2050	11.1641	43.6922
	0.8	0.4000	1.7200	7.7746	26.0790
	0.7	0.3499	1.2949	5.1505	14.3765
	0.6	0.3000	0.9299	3.1940	7.0983
	0.5	0.2500	0.6250	1.8072	2.9713
	0.4	0.1999	0.3799	0.8926	0.9360
	0.3	0.1500	0.1949	0.3523	0.1467
	0.2	0.0999	0.0700	0.0886	−0.0289
	0.1	0.0499	0.0049	0.0037	−0.0094
$\frac{3}{2}$	1.0	2.5000	73.7500	2037.754	52417.86
	0.9	2.2499	59.6248	1481.913	34094.69
	0.8	1.9999	47.0000	1037.433	21044.66
	0.7	1.7499	35.8750	691.883	12145.87
	0.6	1.4999	26.2500	432.849	6411.01
	0.5	1.2500	18.1250	247.911	2986.31
	0.4	0.9999	11.5000	124.650	1151.82
	0.3	0.7499	6.3749	50.646	321.39
	0.2	0.4999	2.7500	13.483	42.67
	0.1	0.2499	0.6250	0.740	−2.87

stiffness, i.e., it increases with a decrease in the spin-wave stiffness, one might interpret the present results as also indicating that whenever randomness is increased a softening of the magnetic system occurs against magnetic field perturbations with wave vectors close to the relevant $\vec{Q}$ vectors. Moreover, the rate of this softening is faster than the rate of reduction of the critical temperature [which is the reason it is noticeable in Figs. 2(a) and 2(b) which are plotted for given ϵ values].

It is interesting to look at the behavior of the susceptibility away from $\vec{k}=\vec{Q}$. Here the corresponding low-temperature observations are again relevant. For example, it is observed[1] that the relative decrease in the spin-wave energy (for a randomly diluted ferromagnet) for $\vec{k}$ vectors near the zone edge (i.e., in the opposite limit to $\vec{k}=\vec{Q}$) is in direct contrast to the $\vec{k}-\vec{Q}=0$ case, i.e., it is much slower than the rate of dilution. Again, we find that an analog for this phenomenon, at $T>T_C$, exists and that (see Fig. 3), as one proceeds away from $\vec{k}=\vec{Q}$, the relative susceptibility for the random system becomes smaller than that corresponding to the pure system. For different relative temperatures, the cross over occurs at different $\vec{k}$ values (and indeed for infinite temperature no changes occur at all).

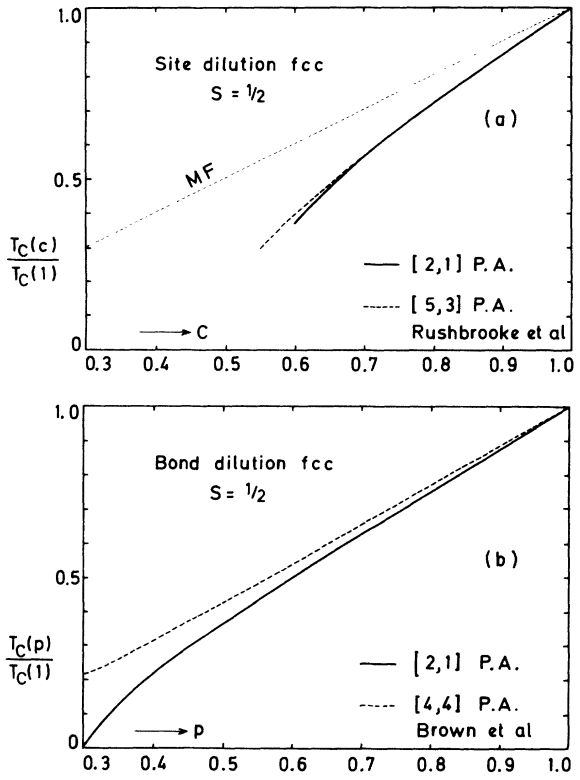

FIG. 1. (a) For the quenched, site-diluted fcc ferromagnet with $S=\frac{1}{2}$, the normalized Curie temperature, $T_C(c)/T_C(1)$, is plotted as a function of the magnetic concentration c. The thick unbroken curve is obtained by using the [2,1] Padé on the present short series, the broken curve shows the result of [5,3] Padé approximant on the longer series given by Rushbrooke *et al.* (Ref. 5). The corresponding mean-field, virtual-crystal approximation result, marked MF, is a straight line which lies higher throughout. (b) This figure corresponds to (a) with the difference that here exchange bonds are diluted. The broken curve shows the results of Brown *et al.* (Ref. 6) using a [4,4] Padé on a much longer series.

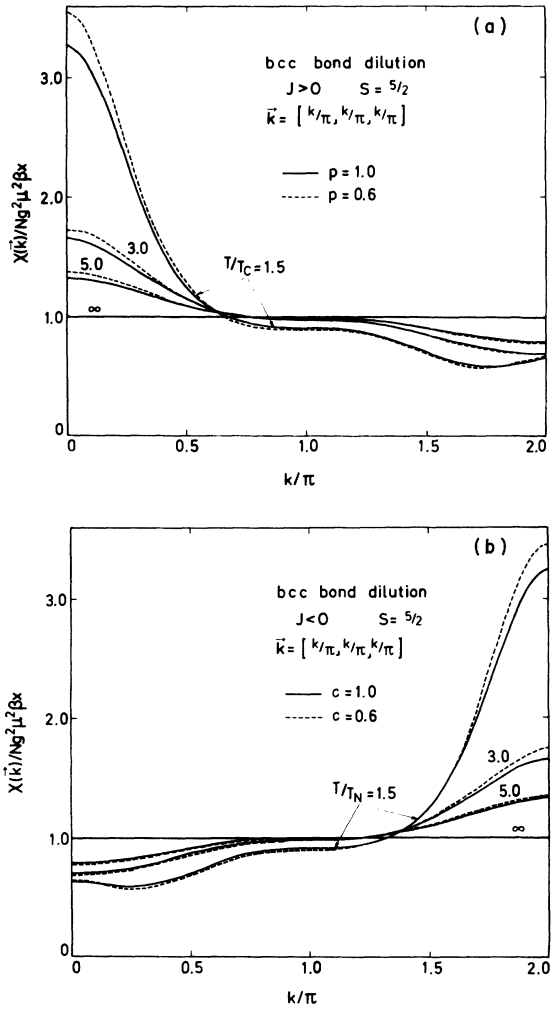

FIG. 2. (a) Generalized susceptibility, for the bcc lattice for $J>0$ with $S=\frac{5}{2}$ and bond dilution, is normalized at $T=\infty$ and is plotted as a function of k/π, where $\vec{k}=(k,k,k)$. The curves for the nonrandom case, $p=1$, are drawn continuously while the broken curves are for magnetic bond concentration $p=0.6$. The appropriate T/T_C values are marked. (b) Same as (a) with the difference that here we have a site random system, i.e., c instead of p, and a negative J and $\vec{k}=(k,0,0)$.

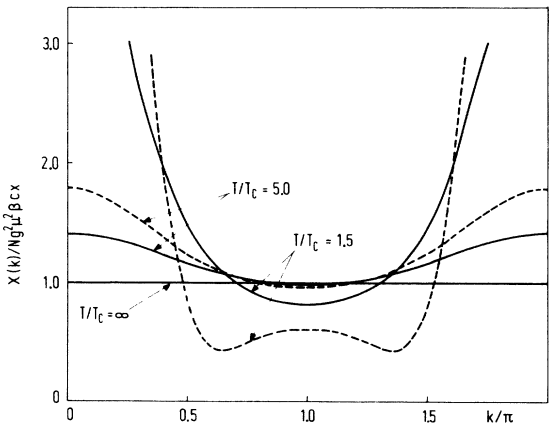

FIG. 3. Same as in Fig. 2(b) except for the difference that here we have an fcc lattice with $S=\frac{1}{2}$ and we are dealing with a site-diluted system, with $c=0.7$ and $c=1.0$ and $J>0$.

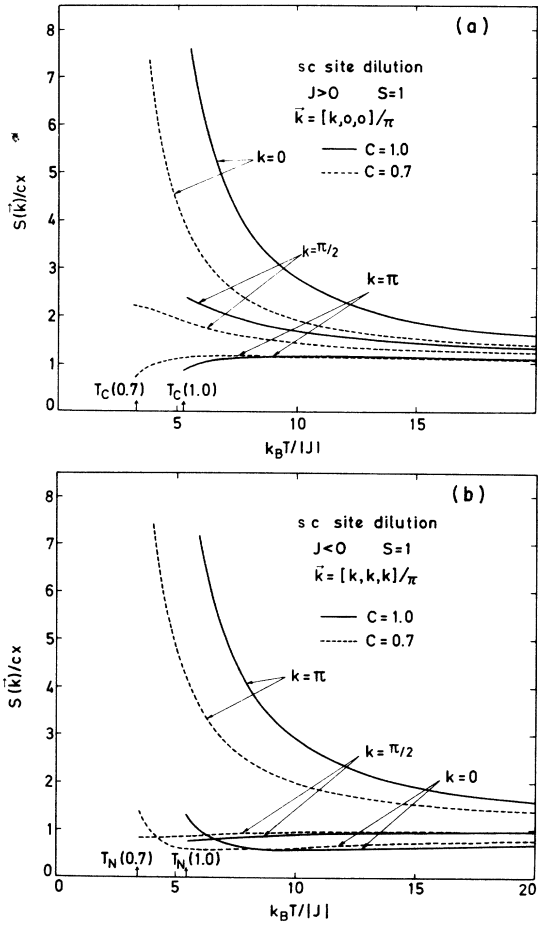

FIG. 4. (a) $S(k)$ is given for a site-diluted system as a function of $k_BT/|J|$ for a simple cubic lattice with $\vec{k}=(k,0,0)$, $S=1$, and $J>0$. The relevant k values are marked. Continuous curves are for $c=1$ and broken curves for $c=0.7$. The correlation function is normalized at $T=\infty$. (b) Same as (a) with the difference that here $\vec{k}=(k,k,k)$ and $J<0$.

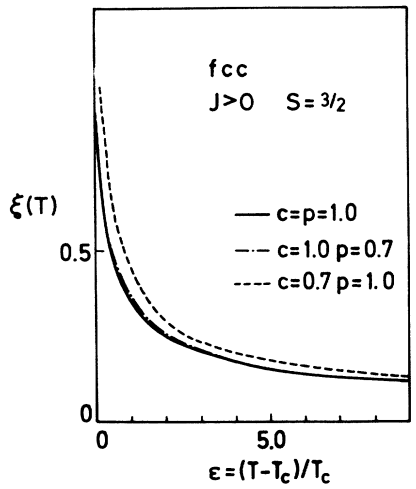

FIG. 5. Effective correlation range is given as a function of the temperature parameter ϵ. The curves are for an fcc lattice with $S=\frac{3}{2}$. Continuous curve is for the pure system; dashed curve for site random system with $c=0.7$; and the dash-dot is for bond random system with $p=0.7$.

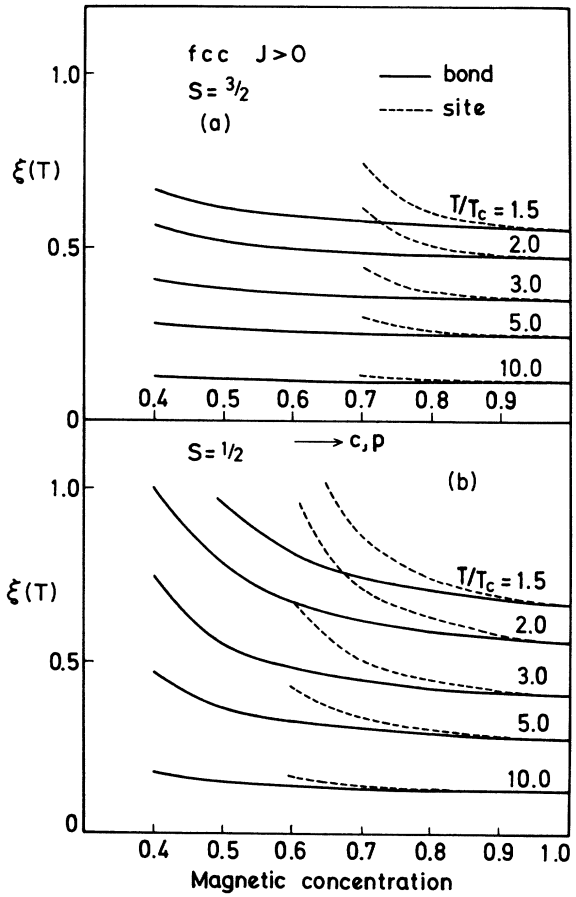

FIG. 6. (a) Effective correlation length is given for several values of T/T_C for site random (continuous curves) and bond random (broken curves) system with $S=\frac{3}{2}$. (b) Same as (a) but with $S=\frac{1}{2}$.

Of course, the behavior of the generalized susceptibility and the correlation function is roughly similar. Therefore for brevity, we do not include the corresponding plots for $S(\vec{k})$. Instead, for completeness, we include Figs. 4(a) and 4(b), where $S(\vec{k})$ for a site-diluted, simple cubic system with positive and negative exchange coupling, respectively, is shown in terms of the unrenormalized units $k_B T/|J|$. Here we notice that excepting for the extremely narrow region in the immediate vicinity of the wave vector furthest from $\vec{k}=\vec{Q}$, i.e., $\vec{k}=0$ for the antiferromagnetic coupling, and temperatures near the transition point of the pure system, the absolute value of the $T\to\infty$ normalized correlation function is smaller for the random lattice. (note that these remarks refer to temperatures where both the pure as well as the random systems are paramagnetic.)

As mentioned earlier, our series is too short to give any meaningful results in the critical region. However, the convergence of the series is reasonable for $T/T_C \gtrsim 2$ and by appropriate extrapolation, such as can be done by the use of Padé representation, we can be reasonably confident that the qualitative features of our results will be meaningful for $T/T_C \sim 1.5$, if not even somewhat closer to T_C. In this spirit, we have analyzed the behavior of the effective correlation length $\xi(T)$ in Figs. 5, 6(a), and 6(b). We notice that for given T/T_C, the effective correlation length is longer for the random system. Also, we notice that this tendency is somewhat more pronounced, for given dilution, for the site-random system. The latter fact is not surprising in view of the fact that percolation concentrations are larger for the site system, i.e., that for given dilution the probability of the occurrence of the infinite cluster is higher in the bond random system. Therefore, effectively the bond random system for given dilution seems to behave like a site-random system of somewhat larger magnetic concentration.

ACKNOWLEDGMENT

We are greatly indebted to Professor M. F. Collins for his active interest in this work and for his many helpful communications.

APPENDIX

The expressions for Σ_n, $n=1,\ldots,4$, i.e.,

$$\Sigma_1=\sum_{\vec{p}}\cos\vec{k}\cdot\vec{p},\quad \Sigma_2=\sum_{\vec{p}}\sum_{\vec{p}_2}\cos\vec{k}\cdot(\vec{p}+\vec{p}_2)(1-\delta_{-\vec{p},\vec{p}_2}),$$

$$\Sigma_3=\sum_{\vec{p}}\sum_{\vec{p}_2}\sum_{\vec{p}_3}\cos\vec{k}\cdot(\vec{p}+\vec{p}_2+\vec{p}_3)(1-\delta_{-\vec{p},\vec{p}_2})(1-\delta_{-\vec{p}_2,\vec{p}_3})(1-\delta_{-\vec{p},\vec{p}_2+\vec{p}_3}),$$

$$\Sigma_4=\sum_{\vec{p}}\sum_{\vec{p}_2}\sum_{\vec{p}_3}\sum_{\vec{p}_4}\cos\vec{k}\cdot(\vec{p}+\vec{p}_2+\vec{p}_3+\vec{p}_4)(1-\delta_{-\vec{p},\vec{p}_2})(1-\delta_{-\vec{p}_2,\vec{p}_3})(1-\delta_{-\vec{p},\vec{p}_2+\vec{p}_3})$$
$$\times(1-\delta_{-\vec{p}_2,\vec{p}_3+\vec{p}_4})(1-\delta_{-\vec{p}_3,\vec{p}_4})(1-\delta_{-\vec{p},\vec{p}_2+\vec{p}_3+\vec{p}_4}),$$

for various lattices of cubic symmetry are as follows:

(a) Simple cubic lattice:

$$\Sigma_1=2(\cos k_x+\cos k_y+\cos k_z),$$

$$\Sigma_2=2[\cos(2k_x)+\cos(2k_y)+\cos(2k_z)]+8(\cos k_x\cos k_y+\cos k_y\cos k_z+\cos k_z\cos k_x),$$

$$\Sigma_3=2[\cos(3k_x)+\cos(3k_y)+\cos(3k_z)]$$
$$+12\{\cos k_x[\cos(2k_y)+\cos(2k_z)]+\cos k_y[\cos(2k_z)+\cos(2k_x)]+\cos k_z[\cos(2k_x)+\cos(2k_y)]\}$$
$$+48\cos k_x\cos k_y\cos k_z+8(\cos k_x+\cos k_y+\cos k_z),$$

$$\Sigma_4=2[\cos(4k_x)+\cos(4k_y)+\cos(4k_z)]$$
$$+16\{\cos k_x[\cos(3k_y)+\cos(3k_z)]+\cos k_y[\cos(3k_z)+\cos(3k_x)]+\cos k_z[\cos(3k_x)+\cos(3k_y)]\}$$
$$+96[\cos(2k_x)\cos k_y\cos k_z+\cos(2k_y)\cos k_z\cos k_x+\cos(2k_z)\cos k_x\cos k_y]$$
$$+24[\cos(2k_x)\cos(2k_y)+\cos(2k_y)\cos(2k_z)+\cos(2k_z)\cos(2k_x)]$$
$$+24[\cos(2k_x)+\cos(2k_y)+\cos(2k_z)]+64(\cos k_x\cos k_y+\cos k_y\cos k_z+\cos k_z\cos k_x).$$

(b) Body-centered-cubic lattice:

$$\Sigma_1 = 8\cos\tfrac{1}{2}k_x\cos\tfrac{1}{2}k_y\cos\tfrac{1}{2}k_z,$$

$$\Sigma_2 = 8\cos k_x\cos k_y\cos k_z + 8(\cos k_x\cos k_y + \cos k_y\cos k_z + \cos k_z\cos k_x) + 8(\cos k_x + \cos k_y + \cos k_z),$$

$$\begin{aligned}\Sigma_3 = {} & 8\cos\tfrac{3}{2}k_x\cos\tfrac{3}{2}k_y\cos\tfrac{3}{2}k_z + 24(\cos\tfrac{3}{2}k_x\cos\tfrac{3}{2}k_y\cos\tfrac{1}{2}k_z + \cos\tfrac{3}{2}k_y\cos\tfrac{3}{2}k_z\cos\tfrac{1}{2}k_x + \cos\tfrac{3}{2}k_z\cos\tfrac{3}{2}k_x\cos\tfrac{1}{2}k_y)\\ & + 72(\cos\tfrac{3}{2}k_x\cos\tfrac{1}{2}k_y\cos\tfrac{1}{2}k_z + \cos\tfrac{3}{2}k_y\cos\tfrac{1}{2}k_z\cos\tfrac{1}{2}k_x + \cos\tfrac{3}{2}k_z\cos\tfrac{1}{2}k_x\cos\tfrac{1}{2}k_y)\\ & + 96\cos\tfrac{1}{2}k_x\cos\tfrac{1}{2}k_y\cos\tfrac{1}{2}k_z,\end{aligned}$$

$$\begin{aligned}\Sigma_4 = {} & 8\cos(2k_x)\cos(2k_y)\cos(2k_z)\\ & + 32[\cos(2k_x)\cos(2k_y)\cos k_z + \cos(2k_y)\cos(2k_z)\cos k_x + \cos(2k_z)\cos(2k_x)\cos k_y]\\ & + 128[\cos(2k_x)\cos k_y\cos k_z + \cos(2k_y)\cos k_z\cos k_x + \cos(2k_z)\cos k_x\cos k_y]\\ & + 24[\cos(2k_x)\cos(2k_y) + \cos(2k_y)\cos(2k_z) + \cos(2k_z)\cos(2k_x)]\\ & + 96\{\cos k_x[\cos(2k_y) + \cos(2k_z)] + \cos k_y[\cos(2k_z) + \cos(2k_x)] + \cos k_z[\cos(2k_x) + \cos(2k_y)]\}\\ & + 72[\cos(2k_x) + \cos(2k_y) + \cos(2k_z)] + 336\cos k_x\cos k_y\cos k_z + 208(\cos k_x\cos k_y + \cos k_y\cos k_z + \cos k_z\cos k_x)\\ & + 112(\cos k_x + \cos k_y + \cos k_z).\end{aligned}$$

(c) Face-centered-cubic lattice:

$$\Sigma_1 = 4(\cos\tfrac{1}{2}k_x\cos\tfrac{1}{2}k_y + \cos\tfrac{1}{2}k_y\cos\tfrac{1}{2}k_z + \cos\tfrac{1}{2}k_z\cos\tfrac{1}{2}k_x),$$

$$\begin{aligned}\Sigma_2 = {} & 8(\cos k_x + \cos k_y + \cos k_z) + 4(\cos k_x\cos k_z + \cos k_y\cos k_z + \cos k_x\cos k_y)\\ & + 16(\cos\tfrac{1}{2}k_x\cos\tfrac{1}{2}k_y\tfrac{1}{2}k_z) + \cos\tfrac{1}{2}k_y\cos\tfrac{1}{2}k_z + \cos\tfrac{1}{2}k_x\cos\tfrac{1}{2}k_z)\\ & + 16(\cos\tfrac{1}{2}k_x\cos\tfrac{1}{2}k_y\cos k_z + \cos\tfrac{1}{2}k_y\cos\tfrac{1}{2}k_z\cos k_x + \cos\tfrac{1}{2}k_x\cos\tfrac{1}{2}k_z\cos k_y),\end{aligned}$$

$$\begin{aligned}\Sigma_3 = {} & 88(\cos\tfrac{1}{2}k_x\cos\tfrac{1}{2}k_y + \cos\tfrac{1}{2}k_y\cos\tfrac{1}{2}k_z + \cos\tfrac{1}{2}k_z\cos\tfrac{1}{2}k_x) + 48(\cos k_x + \cos k_y + \cos k_z)\\ & + 144(\cos k_x\cos\tfrac{1}{2}k_y\cos\tfrac{1}{2}k_z + \cos k_y\cos\tfrac{1}{2}k_z\cos\tfrac{1}{2}k_x + \cos k_z\cos\tfrac{1}{2}k_x\cos\tfrac{1}{2}k_y)\\ & + 48(\cos k_x\cos k_y + \cos k_y\cos k_z + \cos k_z\cos k_x)\\ & + 36[\cos\tfrac{1}{2}k_x(\cos\tfrac{3}{2}k_y + \cos\tfrac{3}{2}k_z) + \cos\tfrac{1}{2}k_y(\cos\tfrac{3}{2}k_z + \cos\tfrac{3}{2}k_x) + \cos\tfrac{1}{2}k_z(\cos\tfrac{3}{2}k_x + \cos\tfrac{3}{2}k_y)] + 48\cos k_x\cos k_y\cos k_z\\ & + 24[\cos k_x(\cos\tfrac{1}{2}k_y\cos\tfrac{3}{2}k_z + \cos\tfrac{1}{2}k_z\cos\tfrac{3}{2}k_y) + \cos k_y(\cos\tfrac{1}{2}k_z\cos\tfrac{3}{2}k_x + \cos\tfrac{1}{2}k_x\cos\tfrac{3}{2}k_z)\\ & \quad + \cos k_z(\cos\tfrac{1}{2}k_x\cos\tfrac{3}{2}k_y + \cos\tfrac{1}{2}k_y\cos\tfrac{3}{2}k_x)] + 4(\cos\tfrac{3}{2}k_x\cos\tfrac{3}{2}k_y + \cos\tfrac{3}{2}k_y\cos\tfrac{3}{2}k_z + \cos\tfrac{3}{2}k_z\cos\tfrac{3}{2}k_x),\end{aligned}$$

$$\begin{aligned}\Sigma_4 = {} & 560(\cos\tfrac{1}{2}k_x\cos\tfrac{1}{2}k_y + \cos\tfrac{1}{2}k_y\cos\tfrac{1}{2}k_z + \cos\tfrac{1}{2}k_z\cos\tfrac{1}{2}k_x) + 304(\cos k_x + \cos k_y + \cos k_z)\\ & + 1088(\cos k_x\cos\tfrac{1}{2}k_y\cos\tfrac{1}{2}k_z + \cos k_y\cos\tfrac{1}{2}k_z\cos\tfrac{1}{2}k_x + \cos k_z\cos\tfrac{1}{2}k_x\cos\tfrac{1}{2}k_y)\\ & + 456(\cos k_x\cos k_y + \cos k_y\cos k_z + \cos k_z\cos k_x)\\ & + 384[\cos\tfrac{1}{2}k_x(\cos\tfrac{3}{2}k_y + \cos\tfrac{3}{2}k_z) + \cos\tfrac{1}{2}k_y(\cos\tfrac{3}{2}k_z + \cos\tfrac{3}{2}k_x) + \cos\tfrac{1}{2}k_z(\cos\tfrac{3}{2}k_x + \cos\tfrac{3}{2}k_y)]\\ & + 576\cos k_x\cos k_y\cos k_z + 416[\cos k_x(\cos\tfrac{1}{2}k_y\cos\tfrac{3}{2}k_z + \cos\tfrac{1}{2}k_z\cos\tfrac{3}{2}k_y) + \cos k_y(\cos\tfrac{1}{2}k_z\cos\tfrac{3}{2}k_x + \cos\tfrac{1}{2}k_x\cos\tfrac{3}{2}k_z)\\ & \quad + \cos k_z(\cos\tfrac{1}{2}k_x\cos\tfrac{3}{2}k_y + \cos\tfrac{1}{2}k_y\cos\tfrac{3}{2}k_x)]\\ & + 96(\cos\tfrac{3}{2}k_x\cos\tfrac{3}{2}k_y + \cos\tfrac{3}{2}k_y\cos\tfrac{3}{2}k_z + \cos\tfrac{3}{2}k_z\cos\tfrac{3}{2}k_x) + 72(\cos 2k_x + \cos 2k_y + \cos 2k_z)\\ & + 192(\cos 2k_x\cos\tfrac{1}{2}k_y\cos\tfrac{1}{2}k_z + \cos 2k_y\cos\tfrac{1}{2}k_z\cos\tfrac{1}{2}k_x + \cos 2k_z\cos\tfrac{1}{2}k_x\cos\tfrac{1}{2}k_y)\\ & + 64[\cos k_x(\cos 2k_y + \cos 2k_z) + \cos k_y(\cos 2k_z + \cos 2k_x) + \cos k_z(\cos 2k_x + \cos 2k_y)]\\ & + 96(\cos k_x\cos\tfrac{3}{2}k_y\cos\tfrac{3}{2}k_z + \cos k_y\cos\tfrac{3}{2}k_z\cos\tfrac{3}{2}k_x + \cos k_z\cos\tfrac{3}{2}k_x\cos\tfrac{3}{2}k_y)\\ & + 48(\cos 2k_x\cos k_y\cos k_z + \cos 2k_y\cos k_z\cos k_x + \cos 2k_z\cos k_x\cos k_y)\\ & + 32[\cos 2k_x(\cos\tfrac{3}{2}k_y\cos\tfrac{1}{2}k_z + \cos\tfrac{3}{2}k_z\cos\tfrac{1}{2}k_y) + \cos 2k_y(\cos\tfrac{3}{2}k_z\cos\tfrac{1}{2}k_x + \cos\tfrac{3}{2}k_x\cos\tfrac{1}{2}k_z)\\ & \quad + \cos 2k_z(\cos\tfrac{3}{2}k_x\cos\tfrac{1}{2}k_y + \cos\tfrac{3}{2}k_y\cos\tfrac{1}{2}k_x)] + 4(\cos 2k_x\cos 2k_y + \cos 2k_y\cos 2k_z + \cos 2k_z\cos 2k_x).\end{aligned}$$

*Supported in part by the NSF under Grant Nos. GH-39023 and DMR-73-07651-A02.
†Supported in part by the U.S. National Academy of Science, Council of Academies of Sciences of Yugoslavia and J. Stefan Institute.

[1]A. Theumann, J. Phys. C 6, 2822 (1973); R. A. Tahir-Kheli, Phys. Rev. B 6, 2808 (1972); 6, 2826 (1972); A. Theumann and R. A. Tahir-Kheli, *ibid.* 12, 1796 (1975).
[2]W. J. L. Buyers, D. E. Pepper, and R. J. Elliott, J. Phys. C 5, 2611 (1972).
[3]L. M. Roth, J. Phys. C 9, L155 (1976).
[4]R. A. Tahir-Kheli and K. Kawasaki, Phys. Rev. B 11, 3413 (1975).
[5]D. J. Morgan and G. S. Rushbrooke, Mol. Phys. 4, 291 (1961).
[6]E. Brown, J. W. Essam, and C. M. Place, J. Phys. C 8, 321 (1975).
[7]M. F. Collins, Phys. Rev. B 2, 4552 (1970); 9, 4996 (1974).